PHYSICAL REVIEW B VOLUME 56, NUMBER 6 1 AUGUST 1997-II

Origin of the polar Kerr effect in PtMnSb and NiMnSb

J. van Ek* and J. M. Maclaren
Department of Physics, Tulane University, New Orleans, Louisiana 70118
(Received 28 February 1997)

The polar Kerr effect for red light reflected from PtMnSb or NiMnSb crystals is shown to be independent of the half-metallic-ferromagnetic property of these compounds. At low photon energies the interband contribution to the Kerr rotation is attributed to transitions between parallel sheets of energy bands that project onto the metallic spin channel. A previously proposed mechanism in which spin-orbit coupling creates an imbalance in optical transitions between states in the vicinity of the Γ point, in the semiconducting minority spin channel, does not apply to either PtMnSb or NiMnSb. Only upon inclusion of intraband effects is reasonable agreement with experiment achieved. [S0163-1829(97)50334-1]

In this paper the relation between the Kerr effect in polar geometry and the details of the electronic structure of PtMnSb and NiMnSb is investigated. These ternary compounds of type $C1_b$ are used as examples in the discussion since they exhibit a relatively large Kerr rotation for red light[1,2] and, at the same time, fall in the class of the half-metallic ferromagnets.[3] In half-metallic ferromagnets, neglecting spin-orbit ($\vec{L}\cdot\vec{S}$) coupling, one spin channel is metallic while the other channel is semiconducting. The coincidence of an exciting Kerr spectrum and the half-metallic-ferromagnetic property quickly led to the conclusion that they must be somehow connected. This resulted in a physically appealing model in which the effect of $\vec{L}\cdot\vec{S}$ coupling on valence states in the semiconducting spin channel, around the Γ point in the Brillouin zone, creates an asymmetry in the optical transitions from those states.[3,4] For PtMnSb, such an imbalance would then result in an unusually large Kerr rotation at photon energies of $\hbar\omega \simeq 1.7$ eV, as observed in experiments.[1] Similar arguments were recently repeated by Oppeneer *et al.*[5]

In this computational study it is shown that this explanation for the Kerr effect does not apply to either PtMnSb or NiMnSb. In addition, the half-metallic-ferromagnetic property is found to be of little relevance for the Kerr effect: at low $\hbar\omega$ the interband-Kerr spectrum is dominated by transitions between parallel sheets of energy bands that cross the Fermi level and that project onto the metallic spin channel.

In what follows the two computational schemes that were employed are briefly discussed. Computed Kerr spectra are then compared with results from experimental and theoretical studies available in the literature. Next, the relation between the electronic structure of the compounds and the Kerr spectrum is analyzed by decomposing the interband contribution to the Kerr angle for low energy photons (i) according to (projected) spin channel, (ii) along high symmetry directions in reciprocal space, (iii) by selective switching of the $\vec{L}\cdot\vec{S}$ interaction, and (iv) by applying hydrostatic pressure to the system.

Two independently developed electronic structure schemes within the local density approximation (LDA) of density functional theory[7] were used. First, the linear muffin tin orbital (LMTO) method within the atomic sphere approximation:[6] For the $C1_b$ structure one empty sphere per formula unit was introduced in the interstitial region in order to reduce the overlap between adjacent atomic spheres. Radii for all atomic spheres were taken to be equal. An LMTO basis including s-, p-, d-, and f-type functions was used on each site. The $\vec{L}\cdot\vec{S}$ interaction was always included in the Hamiltonian while the Dirac equation was solved for the core states. Second, the full potential linear augmented Slater type orbital (FP-LASTO) method[8] eliminates any approximation made with respect to the shape of the effective single-particle potential in the crystal. The interstitial region is treated with reciprocal space techniques. A basis consisting of s-, p-, d-, and f-type functions was used. Electrons in the core states were treated scalar relativistically. $\vec{L}\cdot\vec{S}$ terms were not included self-consistently, but were added to the Hamiltonian when the conductivity tensor is computed.

Matrix elements of the momentum operator between Bloch states are formed in order to calculate the optical conductivity tensor, $\sigma_{\alpha\beta}(\omega)$, as a function of photon frequency, ω, from Kubo's linear response expression, neglecting local field effects.[9–11] A phenomenological relaxation time, τ, that enters the conductivity was taken to be such that $\hbar/\tau = 0.2$ eV. The complex polar Kerr angle is given by (ω dependence is implicit) $\Phi_K = -\sigma_{xy}/[\sigma_{xx}\sqrt{1+(4\pi i/\omega)\sigma_{xx}}] = \phi_K + i\epsilon_K$. The real part, ϕ_K, of the complex angle is the Kerr rotation of the plane of polarization while the imaginary part, ϵ_K, corresponds to the Kerr ellipticity of the reflected light. While interband transitions are accounted for from first principles, the Drude contribution (intraband transitions) to the diagonal elements of the conductivity, $\sigma_0/(1-i\omega\tau_D)$, is included semiempirically. Estimates for the parameters σ_0 and τ_D from optical conductivity measurements were taken from Ref. 12.

Calculated spin and orbital magnetic moments agree well with previously published data.[1,13,14] In the absence of $\vec{L}\cdot\vec{S}$ coupling both NiMnSb and PtMnSb are found to be half-metallic ferromagnets (LMTO as well as FP-LASTO). Theoretical LMTO equilibrium lattice constants for NiMnSb and PtMnSb are about 3% and 2% smaller, respectively, than the experimental values.[1] In what follows calculated results for Kerr spectra are at the experimental lattice constant, unless stated otherwise.

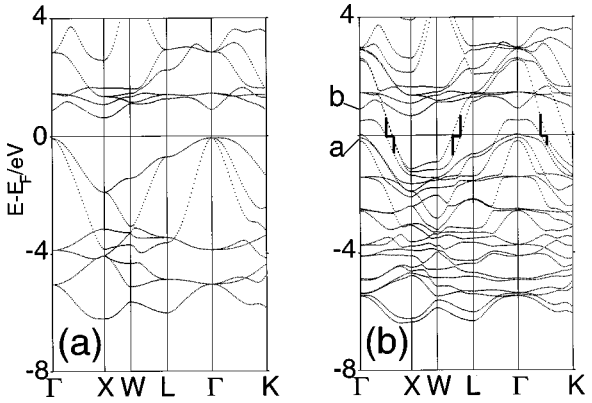

FIG. 1. PtMnSb band structure for (a) the semiconducting spin channel (no $\vec{L}\cdot\vec{S}$ coupling) and (b) the band structure in the presence of $\vec{L}\cdot\vec{S}$ coupling.

Figure 1(a) shows the band structure for the minority semiconducting channel (no $\vec{L}\cdot\vec{S}$ interaction in the band structure calculation). The doubly degenerate flat bands at 1.4 eV above the Fermi level, ϵ_F, are derived from Mn 3*d* states (88%), whereas the highest threefold degenerate set of occupied states at the Γ point are of mixed Pt 6*p* (15%) and Mn 3*d* (70%) character. These occupied states are at the heart of the explanation de Groot *et al.*[3,4] proposed for the large Kerr rotation for red light in PtMnSb. In their view the manifold at Γ splits up under the action of $\vec{L}\cdot\vec{S}$ coupling and this leads to the depopulation of one of the three states, since it is moved up in energy to a value greater than ϵ_F. According to de Groot *et al.* this depopulation results in a severe imbalance in optical transitions from the $\vec{L}\cdot\vec{S}$ split manifold into unoccupied states with $\Delta m_l = \pm 1$.

A look at Fig. 1(b), the band structure for PtMnSb in the presence of $\vec{L}\cdot\vec{S}$ coupling, reveals that the manifold at Γ just below ϵ_F indeed does split. A very small fraction of the states in the highest of the three bands is depopulated as a result of this splitting. However, de Groot *et al.* erroneously took these states to be of Sb 5*p* character, when in reality they are composed of predominantly Mn 3*d* states. Hence, the dipole selection rule $\Delta l = \pm 1$ rules out exceptionally strong vertical transitions between the occupied manifold and the Mn 3*d* states at 1.4 eV above ϵ_F. As it turns out, at low photon energies contributions from the minority spin states in the immediate vicinity of the Γ point to the Kerr spectrum consist of transitions from the three occupied states into the band 1 eV higher in energy, which is a mixture of Pt, Mn, and Sb *s* states.

Figure 2 shows theoretical Kerr rotation spectra for PtMnSb and NiMnSb that were obtained from LMTO and FP-LASTO calculations, as well as experimental data.[1] First, the agreement between the two computational approaches is good: the effect of a full potential treatment is rather limited for PtMnSb and NiMnSb. Second, upon inclusion of the semiempirical Drude term in the conductivity, the experimental trends are clearly reproduced: for PtMnSb a deep minimum for the Kerr angle at photon energies of about 1.5 eV and after that an increasing ϕ_K with increasing $\hbar\omega$ for PtMnSb. For NiMnSb the double minimum structure of ϕ_K is reproduced. Additional structure in $\phi_K(\omega)$ at higher $\hbar\omega$

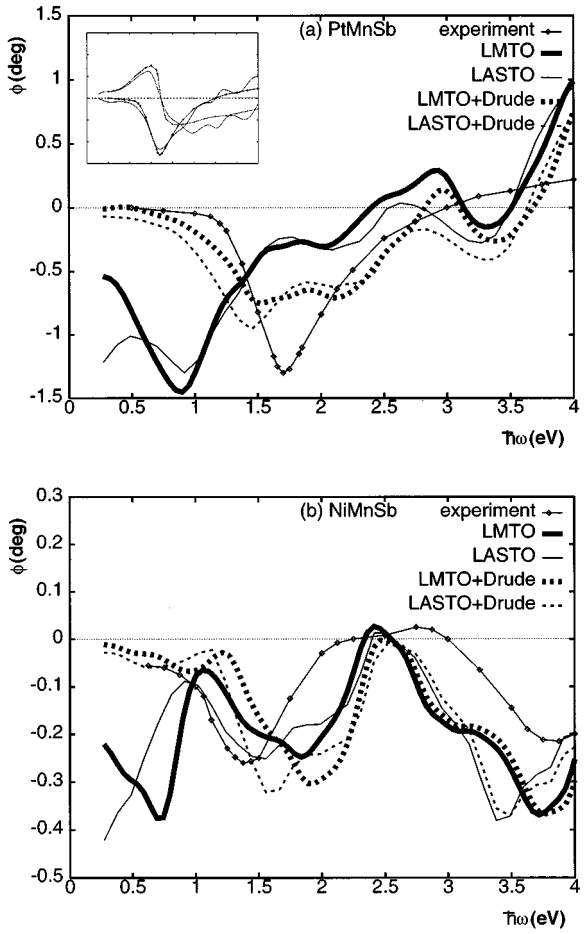

FIG. 2. Computed Kerr rotation for (a) PtMnSb and (b) NiMnSb with the LMTO method and the FP-LASTO method, as well as the experimental results from Ref. 1. The inset in (a) compares theoretical and experimental curves for the Kerr rotation and ellipticity at a smaller lattice constant.

will be affected by energy-dependent lifetime effects that are not taken into account in this study.

In PtMnSb, the intraband conductivity affects the extremum in position ($\hbar\omega \simeq 1.5$ eV) and magnitude ($\phi_K = -0.7°$ to $-0.9°$). Usually the Drude term influences the Kerr spectrum only for energies less than about 1 eV. However, inclusion of the fitted Drude term from Ref. 12 seems to strongly affect the Kerr spectrum over a large part of the visible photon range. Further, it was found that the final Kerr spectrum sensitively depends on the choice for the Drude parameters. Earlier results by Wang *et al.*[13] closely resemble the Kerr rotation (LMTO+Drude) presented in Figs. 2(a) and 2(b). Whereas the results presented here and in Ref. 13 agree very well, those due to Uspenskii *et al.*[15] are somewhat different. For both NiMnSb and PtMnSb these authors compute extremal values for the Kerr effect that are a factor of 2 larger, and that are located at slightly higher photon energies. This may be due to the fact that Uspenskii *et al.* report values for σ_{xx} that are about a factor of 2 smaller than those found in the present study or in Ref. 13.

At this point it must be concluded that for PtMnSb reasonable agreement between theory and experiment can only be achieved upon inclusion of the effect of intraband transitions. With model calculations Feil and Haas[16] illustrated

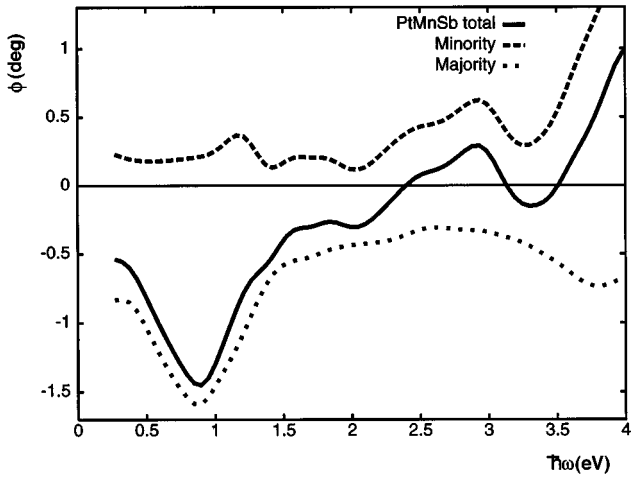

FIG. 3. Approximate projection of ϕ_K onto minority and majority channels for PtMnSb.

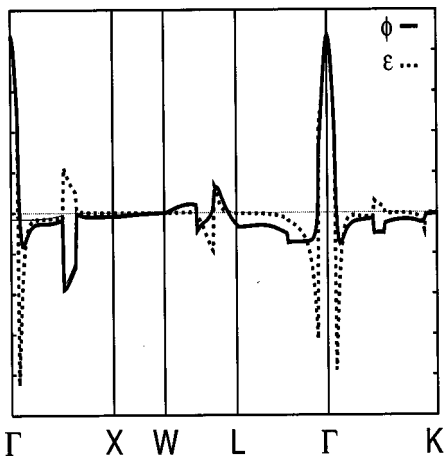

FIG. 4. Contributions to ϕ_K (thick) and ϵ_K (dashed) at $\hbar\omega=0.9$ eV for PtMnSb along high symmetry directions in reciprocal space. The thin solid line along ΓX, which mostly coincides with ϕ_K, shows the contribution from states that project onto the metallic spin channel.

possible enhancement of the Kerr effect in the vicinity of the plasma edge of metals. Feil and Haas only quote the example of PtMnSb, for which there seems to be a big effect, in their paper. However, the diagonal optical conductivity for PtMnSb and NiMnSb behaves very similarly,[12] but *no* strong enhancement due to intraband contributions is observed for NiMnSb.

In the remainder of this paper the focus will be on the contribution from interband transitions to the Kerr effect. Since spin-flip transitions due to a relativistic term in the momentum operator can be safely neglected,[17] a crude distinction between the contributions from minority (semiconducting) and majority (metallic) spin channels can be made. Matrix elements of the momentum operator that enter σ_{xy} were calculated with just the upper or lower half of the vector of LMTO wave function coefficients. Results of this decomposition as well as the complete curve for the Kerr rotation in PtMnSb are shown in Fig. 3. Although this decomposition cannot be rigorously justified, it is clear that for 0.5 eV$<\hbar\omega<$2 eV the Kerr rotation closely follows the contribution from the *metallic* channel. As a matter of fact, the semiconducting channel contributes very little. At higher $\hbar\omega$ the Kerr rotation seems to follow the semiconducting spin channel. It is concluded that the half-metallic property of PtMnSb (and NiMnSb) is not essential for the observed large interband Kerr rotation for red light since the metallic spin channel dominates the Kerr effect at low $\hbar\omega$.

The results of the electronic structure calculations can be analyzed in more detail, providing a deeper understanding of the connection between the band structure and the Kerr effect. For example, Fig. 4 shows contributions to ϕ_K, at $\hbar\omega=0.9$ eV along high symmetry directions in reciprocal space, an energy where the interband contribution peaks. The $\vec{k}$-resolved contributions are defined by $\phi_K(\vec{k}) = -\frac{1}{8}\Sigma_{i=1}^{8}\sigma_{xy}(R_i\vec{k})/[\sigma_{xx}\sqrt{1+(4\pi i/\omega)\,\sigma_{xx}}]$, where the sum is over the eight elements of the magnetic point group $D_{2d}(S_4)$, so that a properly symmetrized tensor is formed. Along ΓX in Fig. 4, the seemingly large contribution to ϕ_K (solid line) at Γ is due to transitions from the three bands labeled ''a'' to band ''b'' in Fig. 1(b), as was found by selectively eliminating transitions in the calculation of $\sigma_{\alpha\beta}$. Contributions from this peak to the integral over the entire Brillouin zone will be modified by a weight roughly proportional to k^2 and, moreover, the sign is opposite to the total computed value for ϕ_K at 0.9 eV. Table I summarizes characters of bands close to ϵ_F at several k points in reciprocal space. Bands ''a'' at Γ are a mixture of Pt-p and Mn-

TABLE I. Dominant atomic orbital character of LMTO energy bands below and above E_F in PtMnSb at selected k points as percentages. The first column indicates the k point and whether the band state projects onto the minority or majority spin channel. The last column gives multiplicity and occupation.

		Pt			Mn			Sb		
k point	6s	6p	5d	4s	4p	3d	5s	5p	5d	
Γ_{min}		15				70				3× occupied
	21			29			33			unoccupied
0.6 ΓX_{maj}	8		28		6	27	9	8		occupied
		10	20		8	23		22		2×unoccupied
0.6 WL_{maj}		6	16		6	34		13		occupied
		11	13		10	23		25		unoccupied
0.5 ΓK_{maj}	6		21			25	7	5		occupied
		9	19			27		17		unoccupied

d, while ''b'' mainly consists of *s* on Pt, Mn, and Sb. Bands ''a'' and ''b'' project onto the semiconducting spin channel [see Fig. 1(b)].

The negative feature in $\phi_K(\vec{k})$ somewhat further along ΓX is associated with a series of transitions between parallel bands that are separated by 0.9 eV, as marked in Fig. 1(b). Optical transitions between these sheets of bands are responsible for the large negative Kerr rotation at 0.9 eV in the theoretical spectrum. Sampling arbitrary radial directions in the three-dimensional Brillouin zone showed that these energy bands form parallel *sheets*, of which the band structure, Fig. 1(b), only shows cross sections. Dominant contributions to the character of the occupied band come from Pt 5*d* and Mn 3*d* states, while the two unoccupied states vertically above it consist of Mn 3*d* and Sb 5*p* states (see Table I). Marked areas along ΓX, WL, and ΓK in Fig. 1(b) contribute to the extremal value of the Kerr rotation, and the character of the bands involved is given in Table I. It was explicitly verified that the excitations away from Γ, which dominate the Kerr spectrum, are associated with states that project onto the *metallic* spin channel (see Fig. 4).

Selectively switching off the $\vec{L}\cdot\vec{S}$ interaction for the different atoms in PtMnSb showed that only $\vec{L}\cdot\vec{S}$ coupling on the Pt site is important for the Kerr spectrum. Hence, spin polarization in the system is provided by the Mn atoms and the effect of $\vec{L}\cdot\vec{S}$ coupling on the Bloch states entirely originates at the Pt site and is conveyed to the magnetic sites by the wave function. In a simplified picture, $\vec{L}\cdot\vec{S}$ coupling in the two spin channels gives rise to equal but opposite contributions to the Kerr effect. Due to the exchange splitting of the bands a net total Kerr effect is observed.

Upon application of hydrostatic pressure to PtMnSb the magnitude of the minimum in the interband-only Kerr rotation increases and is shifted to lower energies, as shown in Table II. The shift towards lower energies is found to correspond to a reduced energy separation between the parallel bands in Fig. 1(b). Interestingly, at $a = 11.02\ a_0$, PtMnSb no longer has the half-metallic property (no $\vec{L}\cdot\vec{S}$ coupling). At the same time ϕ_K is largest (see Table II), demonstrating once more that the half-metallic property is not relevant to the Kerr effect in $C1_b$ Heusler alloys. It is remarkable that, after addition of the Drude intraband term, the agreement between theory and experiment is very good at the smallest lattice constant in Table II [see inset in Fig. 2(a)]. This could point to either surface effects in the experiment or wrong positioning of the bands in the LDA calculation at the experimental lattice constant.

TABLE II. Extremal Kerr rotation at low photon energies in PtMnSb as a function of decreasing lattice constant.

a (a_0)	$\hbar\omega$ (eV)	ϕ_K
11.72	0.90	−1.45°
11.49	0.90	−1.50°
11.25	0.69	−1.54°
11.02	0.53	−1.65°

In conclusion, it was shown that the strong interband-only Kerr effect for low-energy photons in PtMnSb originates from sheets of parallel bands that run through the Brillouin zone. In LDA calculations the parallel bands are separated by about 0.9 eV. These bands predominantly project onto the metallic spin channel. The half-metallic property of PtMnSb is not particularly relevant to the strong Kerr effect. Qualitative agreement between theory and experiment is only achieved upon semiempirical inclusion of a Drude term describing the effect of intraband transitions. An earlier model that attributed great significance to transitions in the semiconducting spin channel, around the Γ point in reciprocal space, does not apply to either PtMnSb or NiMnSb.

This work was supported by the NSF Center for Photoinduced Processes, the Louisiana Board of Regents, and Eastman Kodak Company.

*Electronic address: vanek@circle.phy.tulane.edu

[1] P.G. van Engen, K.H.J. Buschow, R. Jongebreur, and M. Erman, Appl. Phys. Lett. **42**, 202 (1983).

[2] T. Inukai, M. Matsuoka, and K. Ono, Appl. Phys. Lett. **49**, 52 (1986).

[3] R.A. de Groot, F.M. Mueller, P.G. van Engen, and K.H.J. Buschow, Phys. Rev. Lett. **50**, 2024 (1983).

[4] R.A. de Groot, F.M. Mueller, P.G. van Engen, and K.H.J. Buschow, J. Appl. Phys. **55**, 2151 (1984).

[5] P.M. Oppeneer, V.N. Antonov, T. Kraft, H. Eschrig, A.N. Yaresko, and A.Ya. Perlov, Solid State Commun. **94**, 255 (1995).

[6] O.K. Andersen, Phys. Rev. B **12**, 3060 (1975).

[7] W. Kohn and L.J. Sham, Phys. Rev. **140**, A1133 (1965).

[8] G.W. Fernando, J.W. Davenport, R.E. Watson, and M. Weinert, Phys. Rev. B **40**, 2757 (1989).

[9] C.S. Wang and J. Callaway, Phys. Rev. B **9**, 4897 (1974).

[10] P.M. Oppeneer, T. Maurer, J. Sticht, and J. Kübler, Phys. Rev. B **45**, 10924 (1992).

[11] J. van Ek, W. Huang, and J.M. MacLaren, J. Appl. Phys. **81**, 5429 (1997).

[12] P.A.M. van der Heide, W. Baelde, R.A. de Groot, A.R. de Vroomen, P.G. van Engen, and K.H.J. Buschow, J. Phys. F **15**, L75 (1985).

[13] X. Wang, V.P. Antropov, and B.N. Harmon, IEEE Trans. Magn. **30**, 4458 (1994).

[14] S.J. Youn and B.I. Min, Phys. Rev. B **51**, 10 436 (1995).

[15] Yu. A. Uspenskiĭ, É.T. Kulatov, and S.V. Khalilov, JETP **80**, 952 (1995).

[16] H. Feil and C. Haas, Phys. Rev. Lett. **58**, 65 (1987).

[17] Inclusion of $(\hbar/4mc^2)\vec{\sigma}\times\vec{\nabla}V$ in the momentum operator does not produce any noticeable effect on the Kerr rotation, not even for ferromagnetic fcc Pu.